Chapter 6

The Additional Roles of CapZ in Thin Filament assembly, Myofibril Organization and Motoneuron Patterning

Chapter 6: The additional roles of CapZ in thin filament assembly, myofibril organization and motoneuron patterning

6.1 Summary

In this chapter the role of CapZ in thin filament assembly was investigated. Combined loss of function of CapZ with skeletal fast muscle Tropomodulin 4 (Tmod4) or Nebulin (both regulators of actin thin filament formation) produced severe defects in skeletal muscle development. These results indicate firstly, that either CapZ or Nebulin are required for Z-line integrity. Secondly, CapZ is involved in the formation of nemaline rods that are observed in both the zebrafish Nebulin mutant *buzz off* (*buf*) and the Tmod4 morphant. Finally, Tmod4 rather than CapZ is predominantly responsible for nucleation of actin filaments in zebrafish skeletal muscle. The potential interaction of CapZ with the intermediate filament protein Desmin was also explored. MO knockdown of Desmin in zebrafish embryos produced misaligned and wavy myofibrils, similar to the loss of CapZ in skeletal muscle of the *sne* mutant. Additionally, Desmin was severely reduced in the myofibrils of *sne* mutants. These findings suggest that both proteins have overlapping functions in myofibril stability and organization. In the last section of this chapter the axonal projections of motoneurons are shown to be affected in embryos lacking CapZ, thus CapZ may be involved in motoneuron development.

6.2 Introduction

It has been well established that CapZ is an important factor in actin assembly due to its ability to dynamically cap the barbed end of F-actin (Littlefield et al., 2001; Schafer et al., 1996). Actin dynamics is crucial in maintaining thin filament length in muscle cells cultured *in vitro* (Littlefield et al., 2001). In skeletal muscle, CapZ, Nebulin and Tmod have been proposed to be key elements in regulating actin filament formation and ensuring that each actin filament is the

right length. To determine how CapZ is involved in thin filament formation and integrity *in vivo*, knockdown of CapZα1 in *buf* mutants, or double MO knockdowns of Tmod4 and CapZα1 were performed. All double loss of function experiments were performed in collaboration with Dr Elisabeth Busch-Nentwich.

To establish how loss of CapZ caused lateral misalignment of myofibrils in the *sne* mutant, the potential for this protein to link the Z-line to costameric network was investigated. As highlighted in chapter 1, Desmin has been implicated in maintaining the structural and regulatory organization of the myofibrils, therefore this protein was selected as a candidate for potentially interacting with CapZ. Additionally, the Desmin targeted mouse knock out has a strikingly similar phenotype to the *sne* mutant (Li et al., 1997).

A novel protein involved in neural development, V-1, was recently found to interact with CapZ (Taoka et al., 2003). It was suggested that V-1 regulates dynamics of actin polymerization by its interaction with CapZ. Moreover, it has been proposed that V-1 could also play a role in actin driven cell movement and motility during neuronal development (Fujigasaki et al., 1996; Taoka et al., 1994; Taoka et al., 1992). To investigate the possibility that CapZ may affect neuronal development, motoneurons were examined in Islet-1 GFP transgenic embryos injected with capZα1 MOs.

6.3 Combined loss of function studies of thin filament associated proteins

6.3.1 Loss of Nebulin affects myofibrillar structure and produces nemaline rods

The *buf* mutant was first identified in the ENU mutagenesis screen performed in Tübingen (Granato et al., 1996; Haffter et al., 1996) Dr Elisabeth Busch-Nentwich positionally cloned and analyzed the *buf* mutant, and established that the mutant completely lacked expression of the giant thin filament protein Nebulin. The phenotype of this mutant becomes visible at 2-3 dpf, when the embryos fail to emerge out of their chorions. The mutants have a reduced response when touched and are not as motile as wild-type sibling embryos. By 5 dpf the mutant embryos are thinner and have longer axes (Fig. 6.1A and B).

Phalloidin staining indicated that sarcomeric F-actin had formed and assembled into fibrils in the *buf* mutants, however, accumulations of filament at the myoseptum were observed at 3 dpf and 5 dpf (Fig.6.3B and Fig. 6.2B respectively). Immunostaining of α-actinin did not reveal any major defects in the Z-line of 5 dpf mutants, apart from small accumulations of ectopic α-actinin in the myoseptum (Fig. 6.2F). TEM on skeletal muscle sections of 5 dpf mutant embryos indicated that in many places the sarcomeric architecture was still preserved and M-lines, Z-lines, A and I-bands were observed, although the Z-lines were wider than wild-type siblings (Fig. 6.2M and N inset). The ultrastructural analysis also revealed the presence of nemaline rods and large accumulations of ectopic filament (it was not clear whether this was myosin or actin filament) (Fig. 6.2J and N). This phenotype is similar to human patients with nemaline myopathy that have defects in the nebulin gene (Pelin et al., 1999). At 3 dpf fewer nemaline rods were observed by TEM in the *buf* mutants (Dr Elisabeth Busch-Nentwich, personal communication), which suggests that the muscle phenotype is progressive. The phenotypic analysis of the *buf* mutant

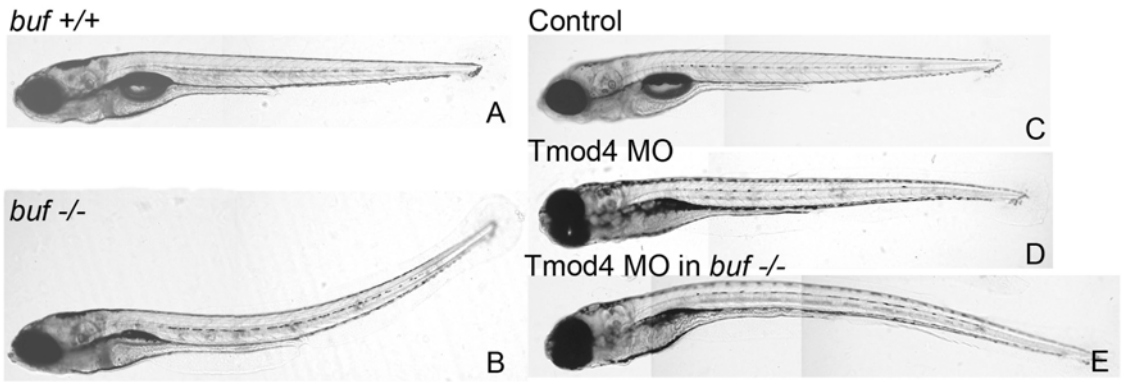

Fig. 6.1. Live images of 5 dpf *buf* and Tmod4 MO injected embryos. A) wild-type sibling, B) *buf* mutant, C) buffer injected control, D) embryo injected with 3ng of Tmod4 MO, E) *buf* mutant injected with 3ng of Tmod4 MO.

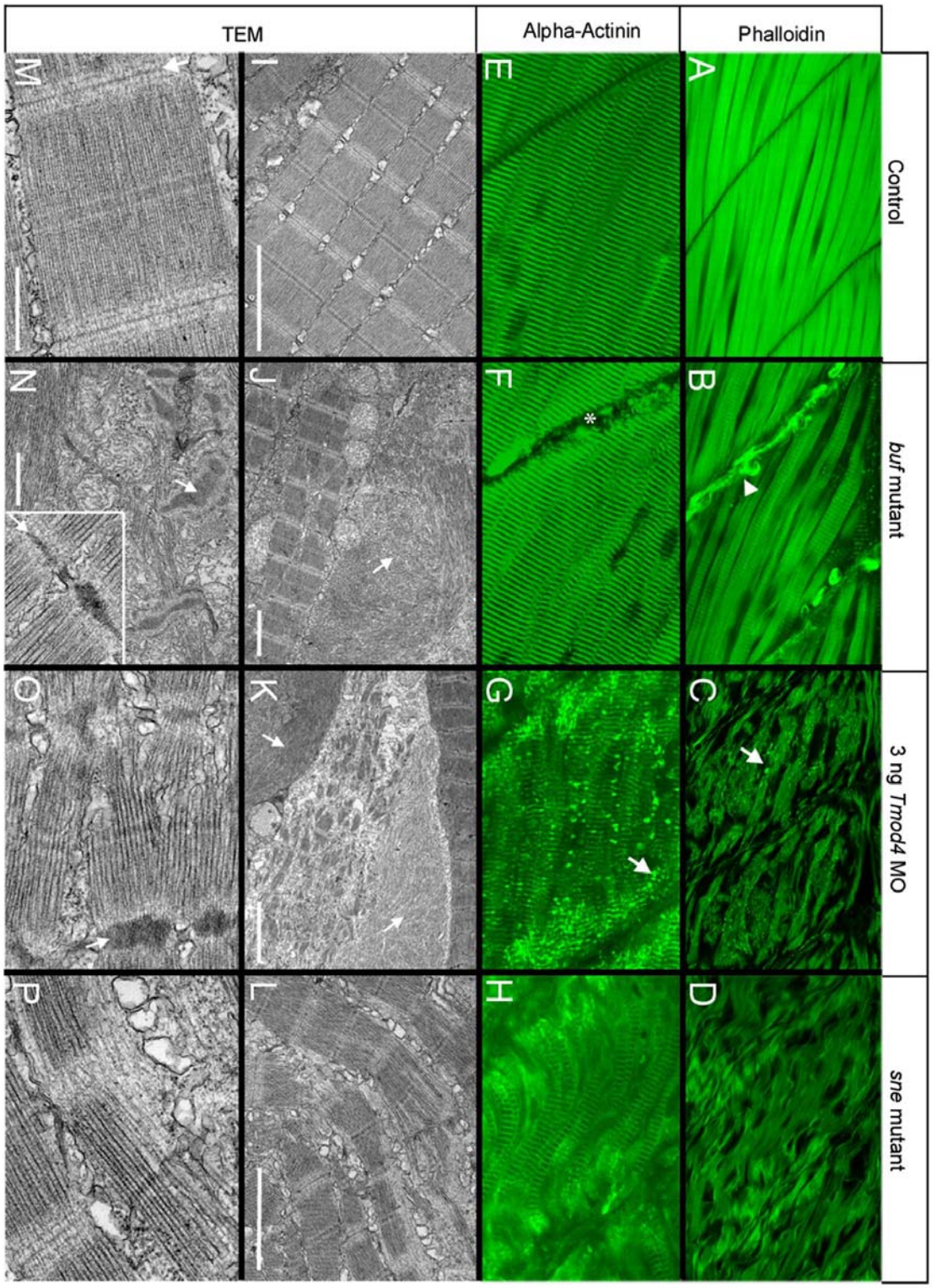
Phalloidin
Alpha-Actinin
TEM
Control
buf mutant
3 ng Tmod4 MO
sne mutant
A
B
C
D
E
F
G
H
I
J
K
L
M
N
O
P

Fig. 6. 2

Fig. 6.2. Phalloidin and α-actinin immunostaining of skeletal muscle in addition to TEM images of day 5 *buf* mutant, *sne* mutant and Tmod4 morphant embryos. A, E, I and M) control, B, F, J and N) *buf* mutant, C,G, K and O) embryo injected with 3ng of Tmod4 MO, D, H, L and P) *sne* mutant. A-D) Phalloidin staining, E-H) α -actinin staining, I-P) TEM images. Scale bar = 2μm for I, J and L, 4μm for K, 500nm for M, inset in N, and P and 1μm for N. Arrowhead in B points to accumulations of actin filament at the myoseptum. Arrow in C points to fragmented actin filaments. Asterisk in F indicates aggregates of α -actinin at the myoseptum. Arrow in G points to punctuate accumulations of α -actinin adjacent to the myoseptum. Arrows in J and K point to ectopic swirls of filament. Arrows in M and N inset point to the Z-line and arrow in N and O indicates the nemaline bodies.

therefore indicates that Nebulin is not essential for initial sarcomere assembly, however, is likely to play a role in maintaining the integrity of the sarcomere structure.

6.3.2 Knock down of Tmod4 produces a similar phenotype to the *buf* mutant

Tmod4 has a similar function to CapZ in that it caps the actin filament, however, it does so at the pointed end, close to the M-line. Littlefield and colleagues (2001) have shown that E-Tmod (Tmod-1) is the primary site for actin filament nucleation, rather than CapZ in cultured chicken cardiomyocytes. Therefore it was not surprising that loss of fast muscle Tmod4 using 3ng of MO targeted to the ATG produced pronounced muscular defects in injected embryos (analysis of the Tmod4 morphant was performed by Dr Elisabeth Busch-Nentwich). At 48 hpf morphants had reduced motility and had failed to come out of their chorions by day 3. On day 5, Tmod4 morphant embryos had longer axes than control embryos and their swim bladders had not inflated (Fig. 6.1D).

Phalloidin staining of day 5 Tmod4 morphant embryos indicated that F-actin was greatly reduced and very few fibrils spanned across each somite (Fig. 6.2C). Immunostaining of α-actinin indicated that Z-lines had formed, however, additional punctate accumulations of α-actinin were also observed that were especially prevalent at regions close to the myoseptum (Fig. 6.2G). TEM images of day 5 muscle sections showed that in many regions the sarcomere structure had collapsed in the Tmod4 morphants (Fig. 6.2K), however, there were still some areas where the sarcomere structure was preserved to some extent, and M-line, Z-line, A-band and I-bands were visible (Fig. 6.2O). Intriguingly, as in the *buf* mutant, nemaline rods and swirls of thick and thin filament (Fig. 6.2K arrows) were also observed.

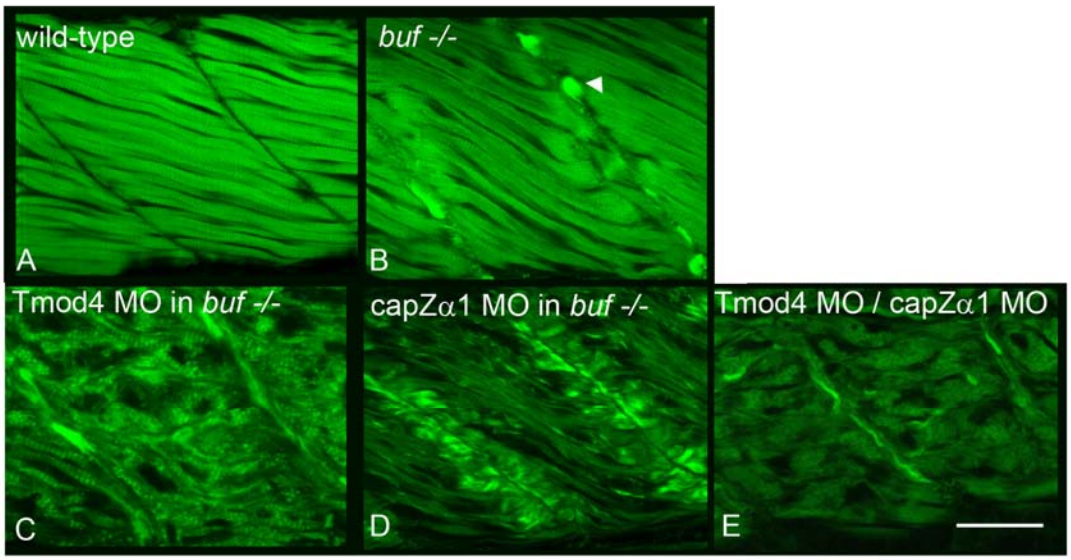

Fig. 6.3. Phalloidin staining of 3 dpf double loss of function embryos. A) wild-type sibling, B) *buf* mutant, arrowhead indicates accumulation of actin filament at the myoseptum C) *buf* mutant injected with 3ng of Tmod4 MO, D) *buf* mutant injected with 10ng of capZα1 splice 2 MO, E) embryo co-injected with 3ng of Tmod4 MO and 10ng of capZα1 splice 2 MO. Scale bar = 44.36 μm.

6.3.3 Loss of CapZ (by MO knockdown) and Nebulin results in loss of the Z-line and thin filament

CapZ, Nebulin and Tmod are thought to be integral in thin filament formation and maintenance. Although the loss of each of these proteins clearly affects muscle function, sarcomere assembly is not completely inhibited as Z-lines and some components of the sarcomere are still visible by day 5. This would suggest that alone each of these proteins are not essential for sarcomere formation, but are required for maintaining the stability and integrity of the muscle tissue as it contracts. However, it is still not known whether *in vivo* the combination of these proteins would be required to establish and maintain thin filaments within the sarcomere.

To observe the effect of loss of Nebulin and CapZ during zebrafish development, 10ng of the capZα1 splice 2 MO was injected into *buf* embryos and the muscle phenotype of these embryos was assessed. On day 3 the motility of the *buf* /CapZα1 double loss of function embryos was severely diminished and they were only able to move the posterior end of their tails when a flight stimulus was provoked. Phalloidin staining at both 3 and 5 dpf showed that actin filaments were severely reduced and there also appeared to be accumulations of actin filament at the myoseptum boundaries (Fig. 6.3D and 6.4D). Moreover, staining with the α-actinin antibody revealed an almost complete loss of α-actinin localization at the Z-line at 5 dpf, however, α-actinin had accumulated ectopically near the myosepta (Fig. 6.4H). TEM images at this stage also confirmed the complete loss of Z-lines (Fig.6.4P arrow) in the *buf* /CapZα1 double loss of function embryos. Surprisingly, the arrangement and localization of thick filament was not affected in what was left of the sarcomere and nemaline bodies were not observed. However, the swirls of ectopic filament as seen in the *buf* only mutants were still present. The absence of Nebulin and CapZ therefore results in loss of thin filaments and Z-lines within sarcomeres.

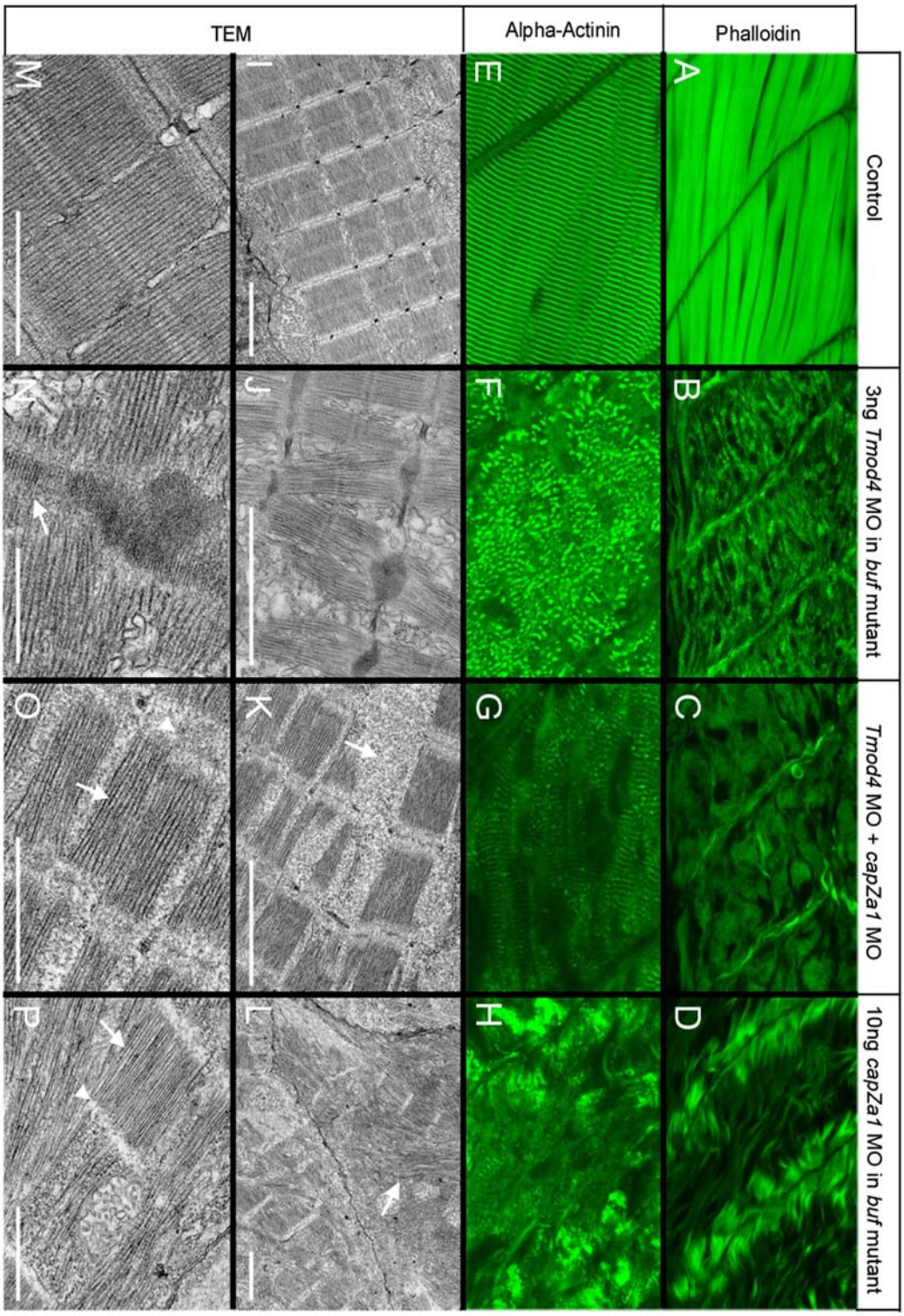
Phalloidin
Alpha-Actinin
TEM
Control
3ng Tmod4 MO in buf mutant
Tmod4 MO + capZa1 MO
10ng capZa1 MO in buf mutant
A
B
C
D
E
F
G
H
I
J
K
L
M
N
O
P

Fig. 6.4

Fig. 6.4. Phalloidin and α-actinin immunostaining of skeletal muscle, in addition to TEM images of day 5 *buf* /capZα1 double loss of function embryos. A, E, I and M) control, B, F, J and N) *buf* mutant injected with 3ng of Tmod4 MO, C,G, K and O) embryo co-injected with 3ng of Tmod4 MO and 10ng of capZα1 splice 2 MO, D, H, I and P) *buf* mutant injected with 10ng of capZα1 splice 2 MO. A-D) Phalloidin staining, E-H) α-actinin staining, I-P) TEM images. Scale bar = 2μm for I, J, K and L, 1μm for M, O, and P, 500nm for N. Arrow in K indicates the absence of a sarcomere. Arrow in L points to swirls of ectopic filament. Arrow in N indicates the nemaline bodies. Arrows in O and P point to the lack of M-line and arrowheads point to the lack of Z-line

6.3.4 *sne/buf* double mutants phenocopy the mutant/morphant knockdown

To confirm the *buf* /CapZα1 double loss of function phenotype, *sne* and *buf* heterozygotes were crossed. The F1s were genotyped for an allelic mutation in *capZα1* and subsequently incrossed to identify carriers that were heterozygous for the *sne* and *buf* mutations. The double mutant embryos phenocopied the *buf* /CapZα1 double loss of function embryos and were virtually immotile by 3 dpf. At 5 dpf the double mutants had shorter axes compared to the *buf* mutants, however, they were still longer than the *sne* mutants or the wild-type siblings (Fig.6.5). α-Actinin antibody staining of day 5 double mutant embryos revealed that very few Z-lines were present and α-actinin had accumulated adjacent to the myoseptum. Phalloidin staining also indicated that virtually no actin filaments had assembled within the myofibres (Fig.6.6A and D). The generation of the *sne*/*buf* mutants therefore supports the results of the double loss of function experiments. However, ideally, TEM analysis will be necessary to completely verify that the double mutants replicate the *buf* /CapZα1 double loss of function phenotype.

The *buf* only mutants produced from the *sne*/*buf* heterozygote cross can be readily distinguished by their gross morphology (Fig. 6.5C). However, when the skeletal muscle of these mutants was stained with phalloidin, wavy actin filaments were detected. Moreover, large clumps of F-actin had accumulated at the myoseptum (Fig. 6.6C). This phenotype differs from the phalloidin immunostaining images of the originally characterized *buf* mutants (Fig. 6.2B) and is more similar to the *sne* mutant phenotype. The unique morphology of these *buf* mutants raises the possibility that in addition to the loss of Nebulin, they are also heterozygous at the *sne* locus. Therefore, perhaps lower amounts of CapZ and a complete lack of Nebulin in these mutants exacerbates the skeletal muscle phenotype. Genotyping will be required to verify this

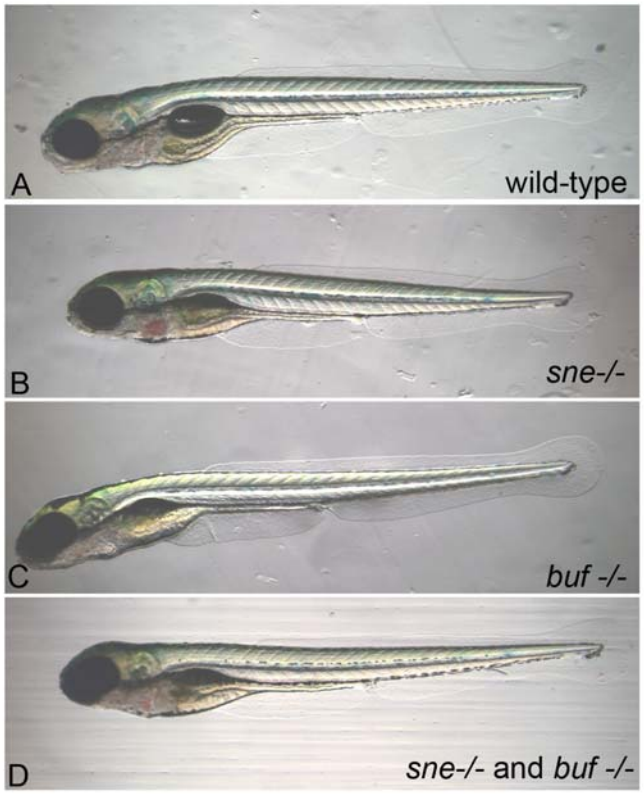

Fig. 6.5. Live images of 5 dpf *sne/buf* mutant embryos. A) wild-type sibling, B) *sne* mutant, C) *buf* mutant, D) *sne/buf* mutant.

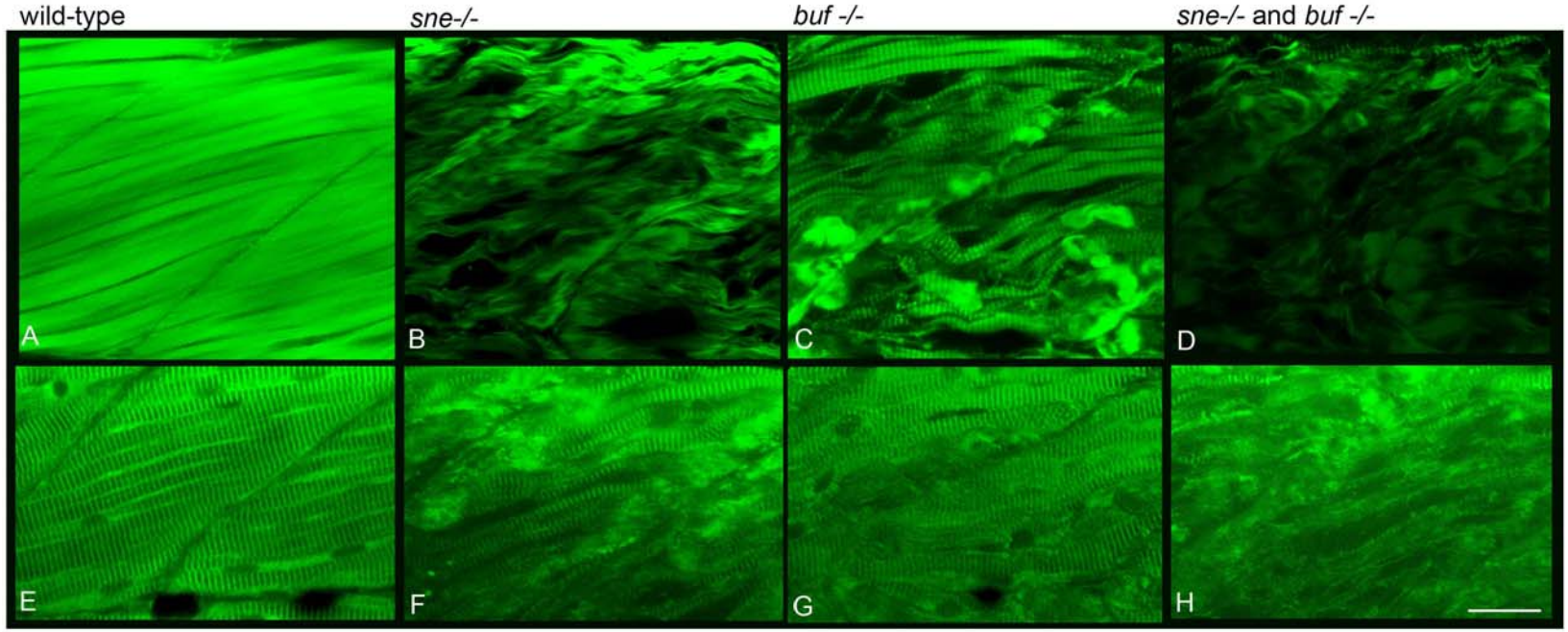

Fig. 6.6. Phalloidin and α-actinin staining of 5 dpf *sne*/*buf* mutant embryos. A-D) Phalloidin staining, E-H) α-actinin staining. A and E) wild-type sibling, B and F) *sne* mutant, C and G) *buf* mutant, D and H) *sne*/*buf* mutant.

interpretation, however, it suggests that levels of CapZ and Nebulin may play an important role in maintenance of the myofibril.

6.3.5 Double MO knockdown of CapZ and Tmod4 completely ablates actin filament and Z-lines

MO injection of 1-2 cell stage embryos with 10ng of capZα1 splice 2 MO and 3ng of ATG Tmod4 MO caused severe muscular defects. On day 3 the double morphants did not move very well and had not emerged from their chorions. Phalloidin staining at this stage revealed that actin filaments were abolished (Fig. 6.3E) and by day 5 they were still not detected (Fig. 6.4C). Although striated Z-lines were visible on day 5, α-actinin levels were dramatically reduced, indicating that many Z-lines had either not assembled or had disintegrated (Fig. 6.4G). TEM analysis of the double loss of function embryos on day 5 confirmed the immunofluorescent stainings. There were very few Z-lines and those that were observed were wider and more diffuse. The sarcomere structure had been partially lost and there was a lack of thin filament, however, thick filament was still observed in ordered blocks even though the Z-line and the thin filament were absent (Fig. 6.4K and O). Unincorporated G-actin also appeared randomly within the myofibril (Fig. 6.4K arrow). Intriguingly, as with the *buf* /CapZα1 double loss of function embryos nemaline rods were not found, however, swirls of ectopic thick filament were still apparent, as seen in the Tmod4 only morphant. These results therefore indicate that *in vivo*, loss of Tmod4 and CapZ completely ablates formation of thin filament and causes Z-line disintegration.

6.3.6 Loss of Tmod4 in *buf* mutants increases the formation of nemaline bodies

Injection of the ATG Tmod4 MO into *buf* embryos produced acute muscle deficiencies that were more severe than loss of Tmod or Nebulin alone. At 3 dpf many of the *buf*/Tmod4

double loss of function embryos had not emerged from their chorions and were almost immotile, and by day 5 had very long axes (Fig. 6.1E). Phalloidin staining on day 3 indicated that virtually no actin filaments had formed within the myofibrils in orderly arrays. Instead, they appeared to accumulate in clumps within the somite (Fig 6.3E), which was also apparent on day 5 (Fig. 6.4B). α-Actinin antibody staining on day 5 identified regions of the somite full of punctuate accumulations of the Z-line protein (Fig. 6.4F). Closer inspection by TEM confirmed that these accumulations were nemaline bodies (Fig. 6.4J and N). Thick filament was also observed between the condensed Z-lines, however, the sarcomeres were randomly orientated and fragmented. Incorporation of thin filament into the distorted sarcomere was also detected and appeared to attach to the nemaline bodies (Fig. 6.4 N). Loss of Tmod4 and Nebulin therefore induces the formation of nemaline bodies from Z-lines, which are likely to result in the complete distortion and fragmentation of the sarcomeric architecture.

6.4 Desmin

Desmin is an intermediate filament costameric protein found in all types of muscle and endothelial cells. Very little is known about the various functions of Desmin in zebrafish development, however, its RNA expression pattern has been characterized (Loh et al., 2000). Whole mount *in situ* hybridization has revealed that *desmin* is expressed in a very similar stage and specific manner to *capZα1*. It is maternally expressed and as development progresses it becomes restricted to the somites, and by 24 hpf it is predominantly expressed in skeletal muscle. The mouse Desmin knockout also produces a strikingly similar phenotype to the *sne* mutant (Li et al., 1997). The muscle myofibres of the soleus and diaphragm became disorganized through progressive muscle use, the myofibrils were wavy and the Z-lines were also not aligned between

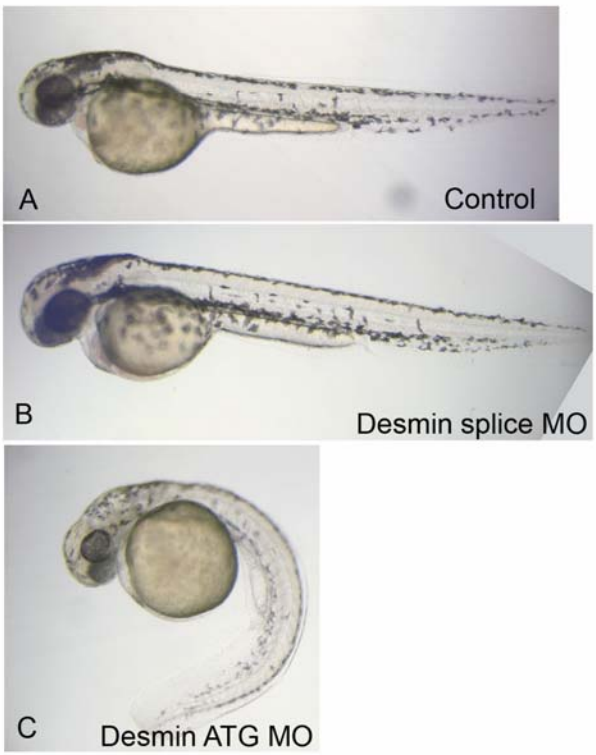

Fig. 6.7. Live images of 2 dpf desmin morphants. A) Buffer injected control, B) embryo injected with 6ng of desmin splice MO, C) embryo injected with 3ng of desmin ATG MO.

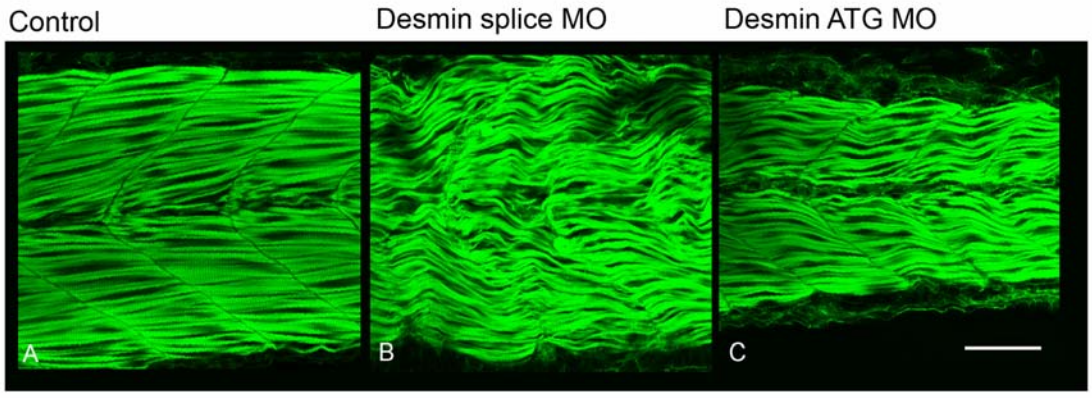

Fig. 6.8. Phalloidin staining of 2 dpf desmin morphants. A) Buffer injected control, B) embryo injected with 6ng of desmin splice MO, C) embryo injected with 3ng of desmin ATG MO.

myofibrils. Other defects included focal degeneration, mitochondrial disorganization and also loss of anchorage of the myofibrils to the plasma membrane at the costamere. Due to the remarkable similarities between the *sne* mutant and the desmin mouse mutant a few experiments were performed to determine whether Desmin and CapZ share functional roles.

6.4.1 Knockdown of Desmin in zebrafish produces wavy myofibres

To examine whether loss of Desmin produced the same phenotype in zebrafish as it did in mice, 6ng of desmin splice MO (targeted against the exon 3 donor splice site) and 3ng of desmin ATG MO were injected into 1-2 cell embryos. By day 2 the splice morphants looked very similar to the wild type controls, however, the ATG morphants were severely affected. The ATG morphant embryos had curved tails, smaller brains, less pigment, and did not respond well to prodding by a mechanical stimulus (Fig.6.7). By day 5, the swim bladders had not inflated in the ATG morphants. Moreover, most injected embryos had shortened axes, heart edemas, smaller brains, and bent tails. The splice MO at this stage was comparable to wild type buffer injected control embryos, the swim bladder had inflated and embryos were swimming normally. Intriguingly, phalloidin staining of day 2 morphants illustrated that wavy myofibres were produced in both the splice and the ATG MO injected embryos (Fig. 6.8). This phenotype is very similar to the phenotype observed with the knock down of CapZα1, and is also similar to what is observed in the Desmin mouse mutant.

6.4.2 Loss of CapZ and Desmin does not enhance myofibrillar disorganization

To determine whether loss of both CapZα1 and Desmin are directly involved in the same mechanism for maintaining myofibrillar integrity, double MO injections were performed to determine whether loss of both these proteins enhanced the wavy phenotype. Both MOs were injected at low doses so that individually each MO only produced a mild phenotype. Embryos

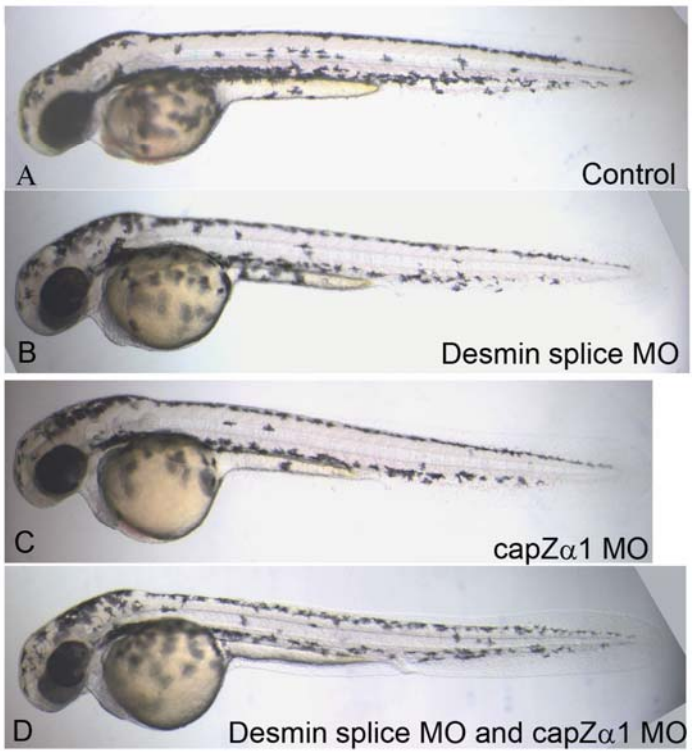

Fig. 6.9. Live images of 2 dpf embryos co-injected with desmin and capZα1MO. A) Buffer injected control, B) embryo injected with 8ng of desmin splice MO,C) embryo injected with 10ng of capZα1 splice 2 MO,D) embryo co-injected with 8ng of desmin splice MO and10ng of capZα1 splice 2 MO.

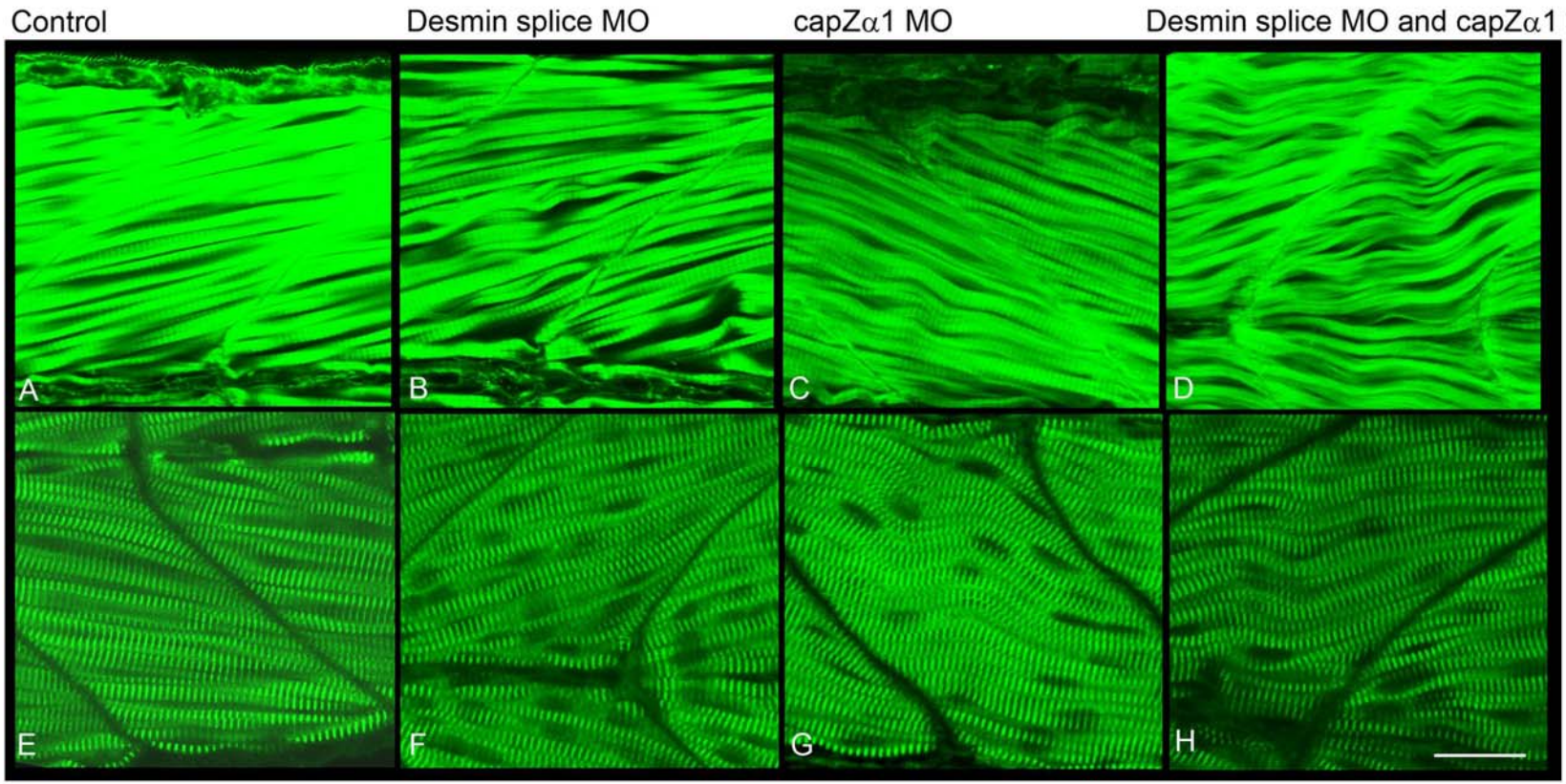

Fig. 6.10. Phalloidin and a-actinin immunostaining of embryos co-injected with desmin and capZa1 MO.A-D) phalloidin, E-H) a-actinin. A and E) Buffer injected control, B and F) embryo injected with 8ng of desmin splice MO,C and G) embryo injected with 10ng of capZa1splice 2 MO, D and H) embryo co-injected with 8ng of desmin splice MO and10ng of capZa1 splice 2 MO. Scale bar = 22.18 mm.

were visualized on day 2, as the effect of the MO tends to decline after three days. 8ng of desmin splice MO and 10ng of capZα1 splice 2 MO were injected separately and co-injected into 1-2 cell stage embryos. On day 2, both individually injected embryos were comparable to the wild type control (Fig. 6.9A, B and C). The overall morphology of the double morphants was very subtle, they had a slightly smaller brain and eyes, however, the tail had extended properly and somites and notochord had formed normally (Fig. 6.9D). Phalloidin staining revealed that the double morphants had slightly wavier fibrils compared to the single morphants, however, no significant difference was observed with α-actinin staining (Fig. 6.10). These results suggest that loss of both Desmin and CapZ does not disrupt the myofibrillar organization in zebrafish embryonic muscle any more than loss of either alone.

6.4.3 Desmin is mis-localized in the myofibrils of *sne* mutants

To determine whether Desmin was affected by loss of CapZ, a polyclonal antibody was used to detect Desmin in the skeletal muscle of 5 dpf *sne* mutant and wild-type sibling embryos. In wild-type sibling embryos Desmin clearly localized to the myoseptum and also appeared to surround each muscle fibre (Fig.6.11). Moreover, within each confocal section a few fibres possessed a distinct striated staining pattern (Fig.6.11A inset). It is possible that this staining pattern is only observed when the confocal scans across a section of tissue that cuts through the edge of the fibril. Alternatively, as this particular staining pattern is not observed uniformly throughout the muscle tissue, the antibody may not be able to penetrate the muscle tissue effectively. Despite the discrepancies in the staining pattern, the control (secondary antibody only) produced virtually no signal. This confirms that the Desmin antibody is specific and the positive staining observed in the myosepta is not an artifact of the accumulation of secondary

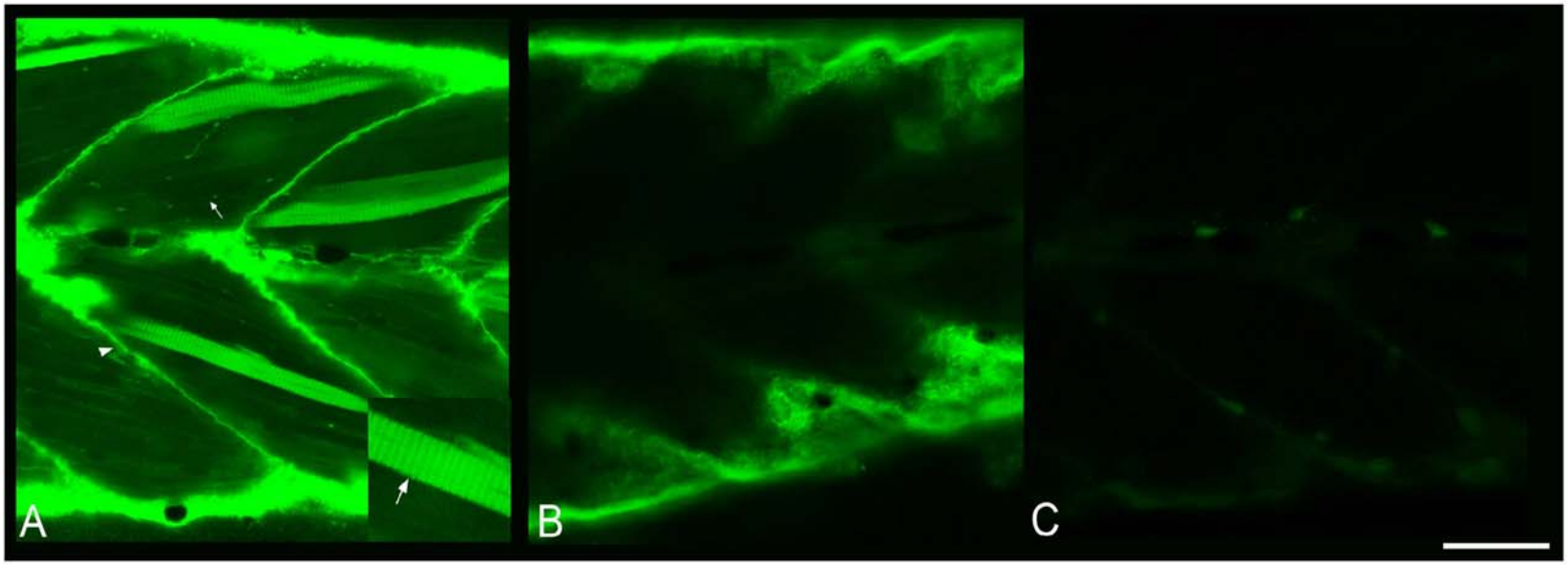

Fig. 6.11. Desmin antibody staining of 5 dpf *sne* mutant and wild-type sibling embryos. A) Wild-type sibling, arrowhead indicates staining in the myoseptum and arrow points to staining around each myofibril. The inset in A is a magnification of the myofibril, illustrating the striated staining pattern (arrow). B) *sne* mutant, C) control (secondary antibody only) on wild-type sibling embryo. Scale bar = 44.36 μm.

antibody. Surprisingly, in the *sne* mutant, staining was absent at the myoseptum. Moreover, Desmin was not detected surrounding the myofibrils or in the characteristic striated pattern that was observed in some of the myofibrils within the wild-type sibling muscle tissue. However, Desmin was still localized to the epithelial layer surrounding the skeletal muscle. These findings suggest that Desmin localization within the muscle is severely affected by lack of CapZ.

6.5 Loss of CapZ affects secondary motoneuronal axon growth

The role of CapZ in neuronal development was initially investigated using transgenic Islet-1 GFP embryos. Islet-1 is a member of the LIM/ homeobox gene family and is expressed in all postmitotic motoneurons early in their development (Appel et al., 1995; Ericson et al., 1992). Transgenic zebrafish expressing an *islet-1* promoter/ enhancer linked to GFP has enabled visualization of cell bodies, main axons, and peripheral branches of motoneurons within cranial and muscle tissues (Higashijima et al., 2000). CapZα1MOs were therefore injected into transgenic Islet-1 GFP embryos to observe the effect of loss of CapZα1on motoneuron development.

Both the ATG (5ng) and splice 2 capZα1 MOs were injected into1-2 cell stage Islet GFP embryos. On day 3, motoneurons were visualized under a fluorescence dissecting microscope. As mentioned in previous chapters, the capZα1 ATG morphants were delayed in development and therefore had smaller brains and eyes compared to the capZα1 splice 2 morphants and the controls, however, no major differences were observed in the cranial motoneurons (Fig. 6.12A and B). There were a reduced number of Islet-1 positive motoneurons along the body axes of ATG morphants on day 3, however, this defect was not observed on day 4 (Fig. 6.13C and D). This observation was probably due to a general delay in development of the ATG morphants. The

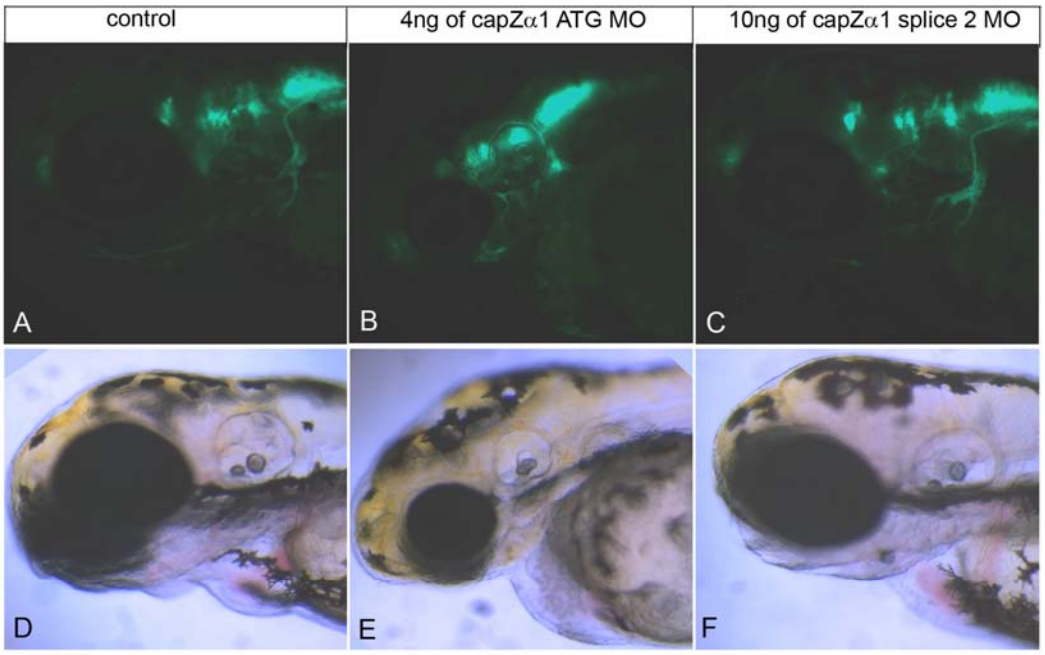

Fig. 6.12. 3 dpf live images of the cranial region of Islet-1 GFP embryos injected with capZα1 ATG or splice 2 MO. A-C) fluorescent images, D-F) bright field images. A and D) Islet-1 GFP control embryo, B and E) Islet-1 GFP embryo injected with 4ng of capZα1 ATG MO, C and F) Islet-1 GFP embryo injected with 10ng of capZα1 splice 2 MO.

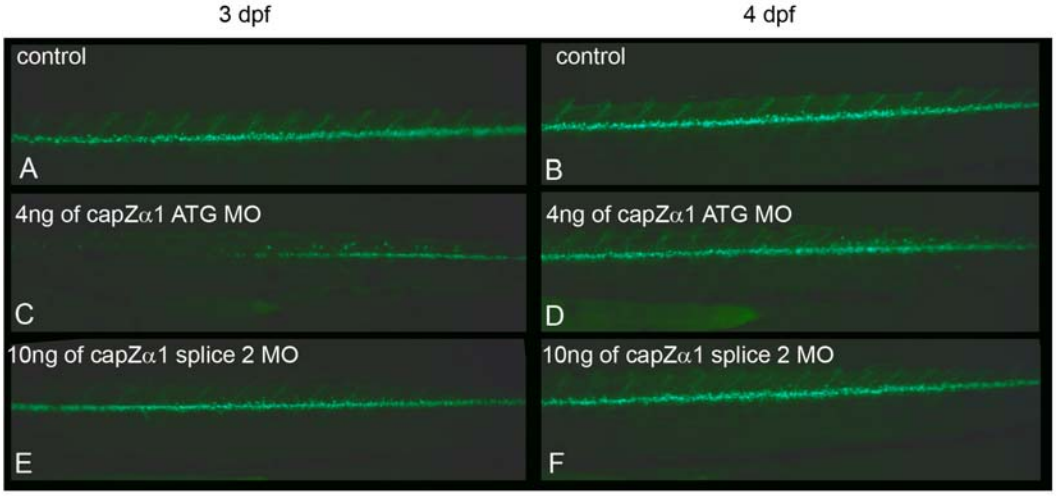

Fig. 6.13.Fluorescent live images of the tail region of Islet-1 GFP embryos injected with capZα1 ATG or splice 1 MO at 3 dpf and 4 dpf. A, C and E) 3 dpf, B, D and F) 4 dpf. A and B) Islet-1 GFP control embryo, C and D) Islet-1 GFP embryo injected with 4ng of capZα1 ATG MO, E and F) Islet-1 GFP embryo injected with 10ng of capZα1 splice 2 MO.

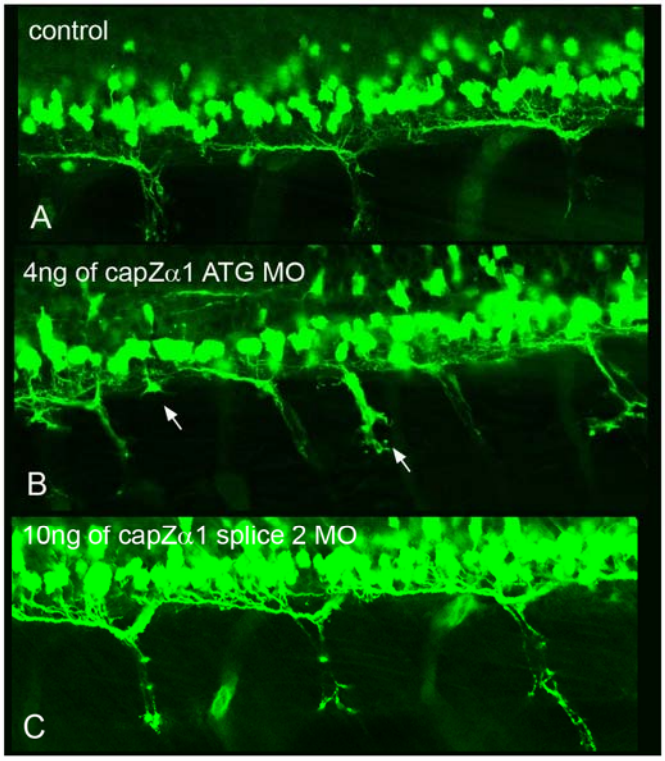

Fig. 6.14. Confocal images of motorneurons from Islet-1 GFP embryos injected with with CapZα1 ATG or splice 1 MO at 5 dpf. A) Islet-1 GFP control embryo, B) Islet-1 GFP embryo injected with 4ng of capZα1 ATG MO, Arrows indicate aberrant axonal projections. C) Islet-1 GFP embryo injected with 10ng of capZα1 splice 2 MO.

formation of motoneurons in the splice 2 morphant was also not defective in the brain or along the spinal cord on day 3 or 4 (Fig. 6.12C and Fig. 6.13E and F). To look in more detail at the axonal projections of the motoneurons within the muscle, confocal imaging of 4 dpf embryos fixed for 2 hrs in 4% PFA was performed (Fig. 6.14). Although the axons had branched and extended into the muscle in the ATG morphants, additional axonal exit points were observed along the spinal cord compared to the control. Moreover, the exit points were also not evenly spaced along the spinal cord (Fig. 6.14B arrows). Aberrant exit points were not observed in the capZα1 splice 2 morphants and therefore indicate that this phenotype is not a non-specific MO effect. Secondary motoneuronal axon projections follow the path of the axons derived from primary motoneurons. Thus it remains to be determined whether the aberrant motoneuron patterning in the ATG capZα1 morphant is due to an initial defect in primary motoneuron axonal growth.

6.6 Discussion

Loss of function of CapZ, in conjunction with other thin filament proteins has indicated that this capping protein clearly plays a major role in maintaining myofibrillar and sarcomeric organization. In this chapter it has been demonstrated that either CapZ or Nebulin are required for maintenance of the Z-lines within the sarcomere. Loss of each of these proteins alone did not affect Z-line stability, however, when both proteins were depleted the Z-lines disassembled. A very small number of intact Z-lines were visualized with α-actinin staining in the *sne*/*buf* double mutants and therefore suggests that in these mutants the Z-line integrity is affected, rather than the initial assembly of the Z-line. Moreover, combined loss of CapZ and Nebulin results in the loss of thin filament. Residual actin filaments were observed by phalloidin staining in day 5 *buf* /CapZα1 double loss of function and double mutant embryos. This observation implies that CapZ and Nebulin are required for stabilizing the actin filament and maintaining it as a polymer.

As expected, loss of both capping proteins completely ablates formation of thin filament. However, the single knockdown of Tmod4 produces a more severe effect in terms of actin filament formation than loss of CapZ, and supports the finding by Littlefield and colleagues (2001) that Tmod is able to nucleate more filaments than CapZ. It is surprising to note that loss of Tmod alone can also affect the morphology of the Z-line, as nemaline bodies very similar to those observed in the *buf* mutant were detected. Tmod could therefore be a novel candidate for causing nemaline myopathies in humans. Intriguingly, CapZ appears to be integral to the formation of nemaline bodies, as knock down of CapZ in both the *buf* mutant and Tmod4 morphants results in loss of nemaline bodies.

In zebrafish, loss of Desmin by MO knockdown induces the formation of wavy myofibres which was very similar to the myofibre phenotype observed in the *sne* mutant. Double knockdowns of Desmin and CapZα1 were performed to determine whether myofibrillar organization was exacerbated by loss of both proteins, however, no obvious effects were observed. In the *sne* mutant, Desmin localization at the sarcolemma and at the myosepta is completely ablated. This suggests that CapZ plays an important role in anchoring Desmin to the Z-line and the myosepta. Moreover, this finding substantiates the CapZα1 /Desmin double knockdown results. As the loss of CapZ alone appears to affect Desmin localization, it is foreseeable that additional loss of Desmin would have no effect on enhancing the existing CapZα1 loss of function phenotype. It will be interesting to determine if CapZ and Desmin directly interact and whether CapZ plays a molecular role in upregulation of Desmin expression. Desmin is an important factor in aligning of the Z-lines between myofibrils and producing a very ordered myofibrillar structure, therefore loss of this protein in *sne* mutants may have a large impact on the phenotype.

In 2003 Taoka and colleagues identified an interaction between CapZ and the neuronally expressed protein V-1 by tandem affinity purification, followed by mass spectrometry. V-1 is expressed in the cerebellum of mice, particularly in the early stages of postnatal development, in the regions where synaptic formation and neuronal migration occur actively during neurogenesis. V-1 inhibited CapZ regulated actin polymerization *in vitro* in a dose dependent manner. In light of this finding the effect of loss of CapZ on neuronal development was investigated.

Motoneurons of transgenic Islet-1 GFP embryos injected with capZα1 MO indicated that the loss of CapZ affected the patterning of axonal exit points from the spinal cord. In wild type embryos only one exit point forms per spinal cord hemisegment, however, in the capZα1 ATG morphants at least two exit points were detected per hemisegment. Spinal motoneurons develop in two waves: The first wave generates three main types of primary motoneurons per hemisegment (CaP, MiP and RoP) and each motoneuron projects axons which leave through a central exit point per hemisegment to innervate the somites. As development proceeds a second wave of motoneurons develop (secondary motoneurons) and extend their axons along the same path as primary axons (For review see (Beattie, 2000)). As the motoneuron defect in the capZα1 morphants was detected on day 4, further experiments will be required to determine whether the loss of CapZ affects primary axonal projections earlier in development. If the primary motoneurons are affected it will be interesting to determine which types of primary motoneuron are forming aberrant axonal projections. Investigation of CapZ's role in motoneuronal development may therefore provide further insight into the mechanisms behind axon growth and intraspinal guidance.